Spin-Orbit Coupling in the Band Structure of Magnesium and other Hexagonal-Close-Packed Metals*

L. M. FALICOV AND MORREL H. COHEN
Institute for the Study of Metals and Department of Physics, University of Chicago, Chicago, Illinois
(Received 30 November 1962)

A calculation of the spin-orbit splitting of the energy levels at the corner of the Brillouin zone in Mg is performed using a six orthogonalized-plane-wave approximation. The parameters of the wave functions were taken from an existing calculation by one of the authors. The corresponding splittings for Be, Zn, Cd, and Tl are estimated from spectroscopic values of the atomic splittings. The changes in the topological properties of the Fermi surface caused by the spin-orbit splitting are discussed as well as the implications of these changes for various physical properties.

I. INTRODUCTION

As has been previously pointed out by the authors,[1] spin-orbit effects modify in an essential way the energy-band picture and the electronic structure of the hexagonal-close-packed (hcp) metals. In particular, the double zone usually employed for these metals must be replaced by the conventional single-zone scheme. The effects are of essential importance in the AHL plane of the Brillouin zone (Fig. 1) where the degeneracy of the energy levels is lifted everywhere except along the AL lines. Here we give a complete account of a calculation for Mg of the splittings at H,[2] where they reach their maximum values. We have used a representation of the wave functions in terms of six orthogonalized plane waves (OPW), twelve considering spin. The values of the orthogonalization coefficients and the potential have been taken from an existing band structure calculation.[3] In Sec. II we discuss the symmetry of the wave functions and their group-theoretical properties. In Sec. III the actual calculation of the splittings in Mg is described. In Sec. IV we discuss the nature of the results and estimate the corresponding values for Be, Zn, Cd, and Tl.

II. SYMMETRY CONSIDERATIONS

We define the direct lattice of a hexagonal structure by the vectors $\mathbf{t}_1$, $\mathbf{t}_2$, $\mathbf{t}_3$, ($\mathbf{t}_4$), where $\mathbf{t}_1$, $\mathbf{t}_2$, and $\mathbf{t}_3$ form a right-handed system, the angles between $\mathbf{t}_1$ and $\mathbf{t}_2$ or $\mathbf{t}_3$ being 90°, the angle between $\mathbf{t}_2$ and $\mathbf{t}_3$, 120° and

$$\mathbf{t}_4=-\mathbf{t}_2-\mathbf{t}_3, \tag{1}$$

$$|\mathbf{t}_1|=c, \quad |\mathbf{t}_2|=|\mathbf{t}_3|=|\mathbf{t}_4|=a. \tag{2}$$

The reciprocal lattice is then defined by the vectors $\mathbf{G}_1\mathbf{G}_2\mathbf{G}_3(\mathbf{G}_4)$, where

$$\mathbf{G}_i=\frac{2\pi\mathbf{G}_j\times\mathbf{G}_k}{\mathbf{G}_i\times\mathbf{G}_j\cdot\mathbf{G}_k}, \quad i,\ j,\ k=1,\ 2,\ 3 \text{ in cyclical order}, \tag{3}$$

$$\mathbf{G}_4=-\mathbf{G}_2+\mathbf{G}_3. \tag{4}$$

The position of the two atoms in the unit cell of the hcp structure are at the origin and at $\boldsymbol{\tau}$, respectively, where

$$\boldsymbol{\tau}=\tfrac{1}{2}\mathbf{t}_1+\tfrac{1}{3}\mathbf{t}_2+\tfrac{2}{3}\mathbf{t}_3. \tag{5}$$

For convenience we also define an orthogonal system of coordinates such that the x axis is parallel to $\mathbf{t}_2$, the y axis parallel to $\mathbf{G}_3$, and the z axis parallel to $\mathbf{t}_1$ and $\mathbf{G}_1$.

To determine the energy levels at the various points of the Brillouin zone, we expand the wave functions of an electron in a series of OPW's,[3-5] defined as

$$|\Psi_{\mathbf{k}\sigma}\rangle=A_{\mathbf{k}}[\Omega^{-1/2}|\exp(i\mathbf{k}\cdot\mathbf{r})\rangle-\sum_{ts}B_{kts}|\Phi_{kts}(\mathbf{r})\rangle]\eta_\sigma, \tag{6}$$

where Ω is the volume of the crystal; $t=1s,\ 2s,\ 2px,\ 2py,\ 2pz,\ \cdots$, etc., indicates the core-electron orbitals; $s=1,\ 2$, denotes the atoms at the origin and at the position $\boldsymbol{\tau}$ within the unit cell, respectively; $\Phi_{kts}(\mathbf{r})$ are the core-electron tight-binding wave functions;

$$B_{kts}=\Omega^{-1/2}\int\Phi_{kts}^*(\mathbf{r})\exp(i\mathbf{k}\cdot\mathbf{r})d^3r \tag{7}$$

are the orthogonalization coefficients;

$$A_{\mathbf{k}}=(1-\sum_{ts}|B_{kts}|^2)^{-1/2} \tag{8}$$

is the normalization coefficient; and η_σ is a spin function.

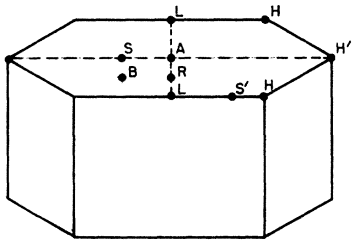

FIG. 1. The Brillouin zone in the hcp structures, showing points and lines of symmetry in the hexagonal face.

* Supported in part by the Office of Naval Research.

[1] M. H. Cohen and L. M. Falicov, Phys. Rev. Letters **5**, 544 (1960).

[2] We must point out that the numerical values given in the last column of Table I in reference 1 as well as the discussion in the paragraph preceding it are in error. The correct values are given in the present paper.

[3] L. M. Falicov, Phil. Trans. Roy. Soc. (London) **A255**, 55 (1962), and thesis submitted to the University of Cambridge, England, 1960 (unpublished).

[4] V. Heine, Proc. Roy. Soc. (London) **A240**, 340, 361 (1957).

[5] T. O. Woodruff, *Solid State Physics*, edited by F. Seitz and D. Turnbull (Academic Press Inc., New York, 1957), Vol. 4, p. 367.

The degeneracies of the levels are given by the dimensions of the irreducible representations of the small group[6] of $\mathbf{k}$ plus the additional degeneracies introduced by time reversal symmetry or accidental degeneracies.[7]

In what follows, when we refer to the degeneracy of a state we include the spin degeneracy, even in the "without-spin" case.

When spin-orbit coupling is neglected, the Hamiltonian for one electron is

$$\mathcal{H}_0 = -(\hbar^2/2m)\nabla^2 + V(\mathbf{r}), \tag{9}$$

and the representations to be considered are those of the so-called "single" group.[8] In particular, we note that for any point of the hexagonal face of the Brillouin zone all the levels are fourfold degenerate[9] and the bands always stick together. This, of course, includes the general point B of the face, whose irreducible representations are given in Table I.[10] The compatibility relations between the relevant representations are given in Fig. 2(a).

When spin-dependent terms are included in the Hamiltonian,

$$\begin{aligned} \mathcal{H}_1 &= \mathcal{H}_0 + \mathcal{H}_{\text{spin}}, \\ \mathcal{H}_{\text{spin}} &= (\hbar/4m^2c^2)(\boldsymbol{\nabla} V \times \mathbf{p}\cdot\boldsymbol{\sigma}), \end{aligned} \tag{10}$$

new irreducible representations must be considered. These are the "double" group representations given by Elliott.[11] In this case we note that only at A, R, and L are the energy levels fourfold degenerate. At the other symmetry points H and S as well as at a general point B, the fourfold degeneracy of the "without spin" case has been lifted and all the levels are now only twofold degenerate. The new compatibility relations are given in Fig. 2(b). It is, therefore, evident that the spin-orbit effects are of fundamental importance in determining the topological properties of the energy surfaces.

We now focus our attention on the point H, where, because of the previous symmetry arguments, the splittings may be expected to reach their maximum value. We consider the twelve OPW's defined by the six $\mathbf{k}$ vectors

$$\begin{aligned} \mathbf{k}_1 &= \tfrac{1}{2}\mathbf{G}_1 + \tfrac{2}{3}\mathbf{G}_2 - \tfrac{1}{3}\mathbf{G}_3, \\ \mathbf{k}_2 &= \mathbf{k}_1 - \mathbf{G}_2, \\ \mathbf{k}_3 &= \mathbf{k}_1 + \mathbf{G}_4, \\ \mathbf{k}_4 &= \mathbf{k}_1 - \mathbf{G}_1, \\ \mathbf{k}_5 &= \mathbf{k}_2 - \mathbf{G}_1, \\ \mathbf{k}_6 &= \mathbf{k}_3 - \mathbf{G}_1, \end{aligned} \tag{11}$$

and both directions of spin. We shall denote these OPW's by $|1\uparrow\rangle$, $|1\downarrow\rangle$, $|2\uparrow\rangle$, $|2\downarrow\rangle$, etc. In the "without spin" case, they transform according to $2H_1+2H_2+2H_3$. The coefficients of the linear combinations transforming according to one given representation can be obtained by the standard projection techniques using the character tables of the representation.[8] These coefficients are given in Table II, where for the sake of clarity we have omitted the spin indices and the normalization factor

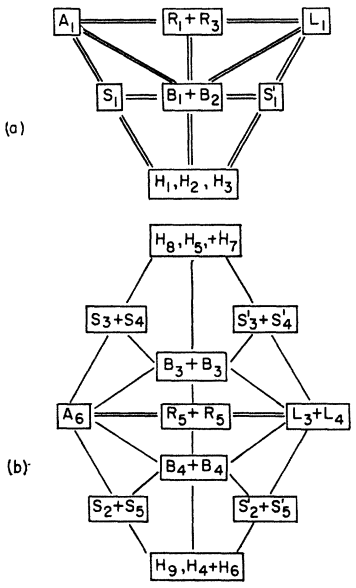

FIG. 2. The compatibility relations between points in the hexagonal face of the Brillouin zone (a) without spin, (b) with spin. Single lines represent double levels and double lines indicate fourfold levels.

TABLE I. Character table of the representations of B.[a]

	Single group		Double group	
	B_1	B_2	B_3	B_4
$(\epsilon\|0)$	1	1	1	1
$(\bar{\epsilon}\|0)$	1	1	-1	-1
$(\rho\|0)$	1	-1	i	$-i$
$(\bar{\rho}\|0)$	1	-1	$-i$	i

[a] Because of time reversal: B_1 and B_2 are degenerate; B_3 and B_4 always occur twice and hence are doubly degenerate.
Characters of elements of the kind $(\alpha|t)$ are obtained by multiplying the character of $(\alpha|0)$ by $\exp(-i\mathbf{k}\mathbf{t})$.

TABLE II. Coefficients of the symmetrized linear combinations of OPW's for the single group at H.[a]

	H_1		H_2		H_3	
	$\|a\rangle$	$\|b\rangle$	$\|c\rangle$	$\|d\rangle$	$\|e\rangle$	$\|f\rangle$
$\|1\rangle$	1	1	1	1	1	1
$\|2\rangle$	w^2	w^2	w	1	w	1
$\|3\rangle$	w	w	w^2	1	w^2	1
$\|4\rangle$	1	-1	-1	1	1	-1
$\|5\rangle$	w^2	$-w^2$	$-w$	1	w	-1
$\|6\rangle$	w	$-w$	$-w^2$	1	w^2	-1
Ion 1	p_x+ip_y	⋯	⋯	s	p_x-ip_y	p_z
Ion 2	⋯	p_x-ip_y	s	⋯	p_z	p_x+ip_y

[a] $w = -\frac{1}{2}+\frac{1}{2}i\sqrt{3}$.

[6] L. P. Bouckaert, R. Smoluchowski and E. Wigner, Phys. Rev. **50**, 58 (1936).
[7] C. Herring, Phys. Rev. **52**, 361, 365 (1937).
[8] C. Herring, J. Franklin Inst. **233**, 525 (1942).
[9] The only exception is the representation A_3, which is eightfold degenerate.
[10] These representations can be trivially derived from reference 8. They are included here for the sake of completeness.
[11] R. J. Elliott, Phys. Rev. **96**, 280 (1954).

TABLE III. Coefficients of the symmetrized linear combinations of OPW's for the double group at H.[a]

Single group	H_1				H_2				H_3			
Double group	H_8		H_9		H_4	H_6	H_8		H_5	H_7	H_9	
$\|1\uparrow\rangle$	1	0	1	0	1	1	1	0	1	1	1	0
$\|2\uparrow\rangle$	w^2	0	w^2	0	w	w	1	0	w	w	1	0
$\|3\uparrow\rangle$	w	0	w	0	w^2	w^2	1	0	w^2	w^2	1	0
$\|4\uparrow\rangle$	1	0	-1	0	-1	-1	1	0	1	1	-1	0
$\|5\uparrow\rangle$	w^2	0	$-w^2$	0	$-w$	$-w$	1	0	w	w	-1	0
$\|6\uparrow\rangle$	w	0	$-w$	0	$-w^2$	$-w^2$	1	0	w^2	w^2	-1	0
$\|1\downarrow\rangle$	0	1	0	1	$-i$	i	0	1	i	$-i$	0	1
$\|2\downarrow\rangle$	0	w^2	0	w^2	$-i$	i	0	w	i	$-i$	0	w
$\|3\downarrow\rangle$	0	w	0	w	$-i$	i	0	w^2	i	$-i$	0	w^2
$\|4\downarrow\rangle$	0	-1	0	1	$-i$	i	0	-1	$-i$	i	0	1
$\|5\downarrow\rangle$	0	$-w^2$	0	w^2	$-i$	i	0	$-w$	$-i$	i	0	w
$\|6\downarrow\rangle$	0	w	0	w	$-i$	i	0	$-w^2$	$-i$	i	0	w^2

[a] $w=-\frac{1}{2}+\frac{1}{2}i\sqrt{3}$.

$6^{-1/2}$. We have designated these linear combinations $|a\uparrow\rangle$, $|a\downarrow\rangle$, $|b\uparrow\rangle$, $|b\downarrow\rangle$, etc.

If we expand these functions in a power series in $\mathbf{r}$ about $\mathbf{r}=0$ and $\mathbf{r}=\boldsymbol{\tau}$, we can determine the angular-momentum character of each of them with respect to the two ion sites of the unit cell in the lattice. We have listed the s- and p-like contribution at the end of Table II.

The inclusion of the spin-orbit term in the Hamiltonian makes the set of our twelve OPW's transform according to $H_4+H_5+H_6+H_7+2H_8+2H_9$, where in fact the initial representations H_1, H_2, and H_3 split in the following fashion:

$$\begin{aligned} H_1 &\rightarrow H_8+H_9, \\ H_2 &\rightarrow H_4+H_6+H_8, \\ H_3 &\rightarrow H_5+H_7+H_9. \end{aligned} \tag{12}$$

The coefficients of the corresponding linear combinations transforming according to each irreducible representation are given in Table III.

Since the pairs H_4-H_6 and H_5-H_7 are degenerate because of time reversal, it is possible to take an arbitrary linear combination of their functions. By doing this we arrive at the simple result for the new linear combinations

$$\begin{aligned} H_4+H_6&: \quad |c\uparrow\rangle, \quad |d\downarrow\rangle, \\ H_5+H_7&: \quad |e\uparrow\rangle, \quad |f\downarrow\rangle, \\ H_{8-1}&: \quad |a\uparrow\rangle, \quad |b\downarrow\rangle, \\ H_{8-2}&: \quad |d\uparrow\rangle, \quad |c\downarrow\rangle, \\ H_{9-1}&: \quad |b\uparrow\rangle, \quad |a\downarrow\rangle, \\ H_{9-3}&: \quad |f\uparrow\rangle, \quad |e\downarrow\rangle, \end{aligned}$$

where the functions in the first column are degenerate with the corresponding functions in the second. We see now that we have been able to separate the two spin systems and consequently deal only with one of them, say the spin-up system. This means that the most important contributions to the spin-orbit splitting will come from those orbital parts with $p_x \pm ip_y$ character, i.e., we expect splittings of the order of the full atomic value for H_1 and H_3 and much smaller values for H_2.

Since the spin splitting of the $3s3p\,^3P_J$ levels in atomic magnesium[12] is 5×10^{-3} eV and the computed[3] energy gaps H_2-H_1, H_1-H_3 for a twelve-OPW basis set (without spin) are 3×10^{-1} and 2.6 eV, respectively, we can compute the crystal spin-splitting by means of first-order perturbation theory, i.e.,

$$\Delta H_1=\langle a\uparrow|\mathcal{H}_{\text{spin}}|a\uparrow\rangle-\langle b\uparrow|\mathcal{H}_{\text{spin}}|b\uparrow\rangle, \tag{13}$$

$$\Delta H_2=\langle c\uparrow|\mathcal{H}_{\text{spin}}|c\uparrow\rangle-\langle d\uparrow|\mathcal{H}_{\text{spin}}|d\uparrow\rangle, \tag{14}$$

$$\Delta H_3=\langle e\uparrow|\mathcal{H}_{\text{spin}}|e\uparrow\rangle-\langle f\uparrow|\mathcal{H}_{\text{spin}}|f\uparrow\rangle. \tag{15}$$

This argument is valid only for light elements, namely, Be, Mg, and probably Zn where the energy gaps are much bigger than the atomic spin splittings. For the heavier elements, Cd and Tl, where both energies are of the same order of magnitude, the mixing of H_1 and H_2 and H_1 and H_3 through their common spin representations H_8 and H_9 must be taken into account and two two-by-two secular equations must be solved. However, estimates of the splittings from their atomic values can be made although they must be considered only an order of magnitude approximation.

III. CALCULATION OF THE SPLITTINGS FOR Mg

To compute (13), (14), and (15) we rewrite $\mathcal{H}_{\text{spin}}$(10) using atomic units ($m=\hbar=1$) and rydbergs (Ry) for the energies

$$\mathcal{H}_{\text{spin}}=(1/4c^2)\mathbf{R}\cdot\boldsymbol{\sigma}, \tag{16}$$

where

$$\mathbf{R}=-i(\nabla V\times\nabla) \tag{17}$$

and V is expressed in Ry.

[12] Charlotte E. Moore, *Atomic Energy Levels*, National Bureau of Standards Circular No. 467 (U. S. Government Printing Office, Washington, D. C., 1949).

TABLE IV. Coefficients of the OPW's, B_{nts}.[a]

n \ t	1s		2s		2px		2py		2pz	
s	1	2	1	2	1	2	1	2	1	2
1	b_1	ib_1	b_2	ib_2	b_3	ib_3	0	0	b_4	ib_4
2	b_1	iw^2b_1	b_2	iw^2b_2	$-\frac{1}{2}b_3$	$-\frac{1}{2}iw^2b_3$	$-\frac{1}{2}\sqrt{3}b_3$	$-\frac{1}{2}i\sqrt{3}w^2b_3$	b_4	iw^2b_4
3	b_1	iwb_1	b_2	iwb_2	$-\frac{1}{2}b_3$	$-\frac{1}{2}iwb_3$	$\frac{1}{2}\sqrt{3}b_3$	$\frac{1}{2}i\sqrt{3}wb_3$	b_4	iwb_4
4	b_1	$-ib_1$	b_2	$-ib_2$	b_3	$-ib_3$	0	0	$-b_4$	ib_4
5	b_1	$-iw^2b_1$	b_2	$-iw^2b_2$	$-\frac{1}{2}b_3$	$\frac{1}{2}iw^2b_3$	$-\frac{1}{2}\sqrt{3}b_3$	$\frac{1}{2}i\sqrt{3}w^2b_3$	$-b_4$	iw^2b_4
6	b_1	$-iwb_1$	b_2	$-iwb_2$	$-\frac{1}{2}b_3$	$\frac{1}{2}iwb_3$	$\frac{1}{2}\sqrt{3}b_3$	$-\frac{1}{2}i\sqrt{3}wb_3$	$-b_4$	iwb_4

[a] $b_1=0.02349$, $b_2=-0.1746$, $b_3=0.09512$, $b_4=0.04394$, $A_n=1.045$, $w=-\frac{1}{2}+\frac{1}{2}i\sqrt{3}$.

Since only spin-up states are involved in the calculation, the only term to be considered is

$$\mathcal{H}_z=(1/4c^2)R_z\sigma_z,$$

$$R_z=-i\left(\frac{\partial V}{\partial x}\frac{\partial}{\partial y}-\frac{\partial V}{\partial y}\frac{\partial}{\partial x}\right), \tag{18}$$

because the other two terms give zero diagonal matrix elements.

We give now a detailed account of the calculation of one of the matrix elements, i.e.,

$$I_a=(1/4c^2)\langle a|R_z|a\rangle. \tag{19}$$

From the considerations of the previous section

$$|a\rangle=\sum_{n=1}^{6}C_{an}|n\rangle$$

$$=A_a[\Omega^{-1/2}\sum_{n=1}^{6}C_{an}|\exp i\mathbf{k}_n\cdot\mathbf{r}\rangle-\sum_{ts}D_{ats}|\Phi_{ts}(\mathbf{r})\rangle], \tag{20}$$

where C_{an} are the coefficients given in Table II,

$$D_{ats}=\sum_{n=1}^{6}B_{nts}C_{an}, \tag{21}$$

and A_a is the new normalization factor.

It is worth noticing that the Bloch tight-binding orbitals are the same for the six **k** vectors under consideration. The coefficients A_n and B_{nts}, and A_i and D_{its} are given in Tables IV and V, respectively. It is evident now that the only matrix elements to be computed are of three different kinds:

$$J_{mn}=\Omega^{-1}\langle\exp(i\mathbf{k}_m\cdot\mathbf{r})|R_z|\exp(i\mathbf{k}_n\cdot\mathbf{r})\rangle, \tag{22}$$

$$K_{n,ts}=\Omega^{-1/2}\langle\exp(i\mathbf{k}_n\cdot\mathbf{r})|R_z|\Phi_{ts}(\mathbf{r})\rangle, \tag{23}$$

$$Q_{ts,t's'}=\langle\Phi_{ts}(\mathbf{r})|R_z|\Phi_{t's'}(\mathbf{r})\rangle, \tag{24}$$

and the main contribution must come from (24).

Integrating by parts, we obtain for (22)

$$J_{mn}=-i(k_{nx}k_{my}-k_{ny}k_{mx})\mathcal{U}(\mathbf{k}_n-\mathbf{k}_m), \tag{25}$$

where

$$\mathcal{U}(\mathbf{G})=\Omega^{-1}\int V(\mathbf{r})\exp(i\mathbf{G}\cdot\mathbf{r})d^3r \tag{26}$$

is a Fourier coefficient of the potential for the reciprocal lattice vector **G**, available from reference 3.

In computing (23) and (24) we assume that the lattice potential $V(\mathbf{r})$ is expressed as a sum of spherically symmetric potentials $U(\rho)$ centered about each atom

$$V(\mathbf{r})=\sum_{\substack{\mathbf{R}_i\text{ lattice}\\ \text{vectors}}}[U(|\mathbf{r}-\mathbf{R}_i|)+U(|\mathbf{r}-\mathbf{R}_i-\boldsymbol{\tau}|)], \tag{27}$$

and that the overlapping of neighboring potentials and core orbitals can be neglected. The last assumption is justified by the results of reference 3. If we now call $\boldsymbol{\varrho}$ the vector going to any point in the crystal from the nearest ion site, we can replace

$$V(\mathbf{r})\to U(\rho),$$

$$\nabla V\to\frac{dU}{d\rho}\frac{\boldsymbol{\varrho}}{\rho}, \tag{28}$$

$$R_z\to-\frac{i}{\rho}\frac{dU}{d\rho}L_z=-\frac{1}{\rho}\frac{dU}{d\rho}\frac{\partial}{\partial\varphi}.$$

TABLE V. Coefficients of the symmetrized combinations of OPW's, D_{its}.

i \ t	1s		2s		2px		2py		2pz		
s	1	2	1	2	1	2	1	2	1	2	A_i
a	0	0	0	0	$(\frac{3}{2})^{1/2}b_3$	0	$i(\frac{3}{2})^{1/2}b_3$	0	0	0	1.014
b	0	0	0	0	0	$i(\frac{3}{2})^{1/2}b_3$	0	$(\frac{3}{2})^{1/2}b_3$	0	0	1.014
c	0	$i6^{1/2}b_1$	0	$i6^{1/2}b_2$	0	0	0	0	0	0	1.109
d	$6^{1/2}b_1$	0	$6^{1/2}b_2$	0	0	0	0	0	0	0	1.109
e	0	0	0	0	$(\frac{3}{2})^{1/2}b_3$	0	$-i(\frac{3}{2})^{1/2}b_3$	0	0	$i6^{1/2}b_4$	1.020
f	0	0	0	0	0	$i(\frac{3}{2})^{1/2}b_3$	0	$-(\frac{3}{2})^{1/2}b_3$	$6^{1/2}b_4$	0	1.020

By expressing the potential $U(\rho)$ in the usual way in atomic theory,

$$U(\rho)=-2\rho^{-1}Z(\rho), \tag{29}$$

we obtain

$$\rho^{-1}dU/d\rho=2\rho^{-3}Z-2\rho^{-2}dZ/d\rho. \tag{30}$$

Values of $2Z$ as obtained from reference 3 and of $2Z'$ and $\rho^{-1}U'$ as computed numerically are given in Table VI. Near the origin (30) diverges as ρ^{-3}.

Finally, if the core orbitals are expressed in the form

$$\Phi_l(\mathfrak{p})=\rho^{-1}P_l(\rho)Y_l(\theta,\varphi), \tag{31}$$

where the Y's are spherical harmonics, we obtain

$$K_{n,x1}=\exp(i\mathbf{k}_n\cdot\boldsymbol{\tau})K_{n,x2}=\frac{3i}{4c^2}\frac{1}{(2r_0^3)^{1/2}}\frac{k_{ny}}{k_n^2}\int_0^\infty P_p(r)\frac{1}{r}\frac{dU}{dr}\left(\frac{\sin k_nr}{k_nr}-\cos k_nr\right)dr, \tag{32}$$

$$K_{n,y1}=\exp(i\mathbf{k}_n\cdot\mathbf{r})K_{n,y2}=-\frac{3i}{4c^2}\frac{1}{(2r_0^3)^{1/2}}\frac{k_{nx}}{k_n^2}\int_0^\infty P_p(r)\frac{1}{r}\frac{dU}{dr}\left(\frac{\sin k_nr}{k_nr}-\cos k_nr\right)dr, \tag{33}$$

$$Q_{x1,y1}=Q_{x2,y2}=Q_{y1,x1}{}^*=Q_{y2,x2}{}^*=-\frac{i}{4c^2}\int_0^\infty[P_p(r)]^2\frac{1}{r}\frac{dU}{dr}dr, \tag{34}$$

where p, x, and y denote $2p$, $2px$, and $2py$, respectively, and r_0 is the radius of the atomic sphere. All other matrix elements are zero in this approximation. The integrals appearing in (32), (33), and (34) have been computed numerically using the values of $P_p(r)$ from reference 3. When all these values are collected and inserted into (19), the values shown in Table VII result for the shifting of the energies and the total spin-orbit splittings.

It is worth noticing that according to the discussion of the previous section, the splittings at H_1 and H_3 are of the order 5×10^{-3} eV and the corresponding value is three orders of magnitude smaller for H_2. It must be pointed out, however, that the smallness of the H_2 splitting is due to the exact cancellation of the p-like contributions to the wave functions $|c\rangle$ and $|d\rangle$. This cancellation only occurs precisely at the symmetry point H; in the neighborhood of H_2 on the AHL plane, the wave functions must have some p character which will produce again a spin-orbit splitting of the order of the atomic value. Therefore, while the values of the splitting are maxima at H_1 and H_3, H_2 is a point of sharp local minimum.

TABLE VI. Values of the potential and its derivative.

ρ	$2Z$	$2Z'$	$\rho^{-1}U'(\rho)$
0.00	24.000	−63.78	∞
0.005	23.681	−63.58	1.92×10^{8}
0.01	23.364	−62.82	2.40×10^{7}
0.02	22.746	−61.12	3.00×10^{6}
0.04	21.570	−57.06	3.73×10^{5}
0.10	18.723	−39.26	2.27×10^{4}
0.20	14.017	−29.71	2.50×10^{3}
0.30	12.096	−21.86	6.91×10^{2}
0.40	10.139	−17.30	2.67×10^{2}
0.60	7.654	−7.62	5.72×10
0.80	7.389	−1.44	1.67×10
1.00	0.876	+16.85	-1.60×10
1.20	2.086	+0.14	1.11
1.60	1.686	−1.26	9.04×10^{-1}
2.00	1.226	−0.95	3.91×10^{-1}
2.60	0.713	−0.76	1.53×10^{-1}
3.40	0.218	−0.40	4.01×10^{-2}
4.20	0.005	−0.12	6.87×10^{-3}
5.00	0.000	0.00	0.00

IV. DISCUSSION

The main effect of the spin-orbit coupling is the removal of the degeneracy of the band for most points of the hexagonal face of the Brillouin zone. This affects in various ways the physical properties of the hcp metals.

No fundamental change is required for the existing theories of alloys. The overlap of the electron distribution into the second and fourth zone generally starts at the points A and L, respectively, where the splittings vanish.

On the other hand, all those properties which depend on the local or topological features of the Fermi surface, e.g., the transport phenomena in the presence of a magnetic field, are essentially changed. Since the bands no longer stick together at an arbitrary point of the hexagonal face, the double-zone scheme ordinarily used in the representation of the energy surfaces ceases to be valid, and new kinds of connectivities appear when the energy surfaces are plotted in the usual single-zone repeated zone scheme. For instance, the piece of the

TABLE VII. Values of the energies for the various levels.

Symmetry without spin	Energy without spin (Ry)	Symmetry with spin	Spin-up wave function	Energy shift I_i (Ry)	Spin splitting (eV)
H_1	0.708	H_8	$\|a\rangle$	2.08×10^{-4}	5.65×10^{-3}
		H_9	$\|b\rangle$	-2.08×10^{-4}	
H_2	0.686	H_4+H_6	$\|c\rangle$	2.76×10^{-7}	7.50×10^{-6}
		H_8	$\|d\rangle$	-2.76×10^{-7}	
H_3	0.898	H_5+H_7	$\|e\rangle$	-2.10×10^{-4}	5.72×10^{-3}
		H_9	$\|f\rangle$	2.10×10^{-4}	

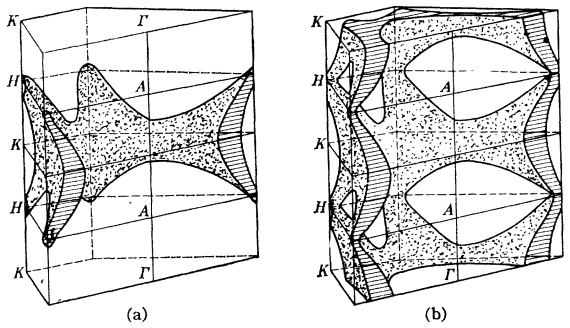

FIG. 3. The change in the connectivity properties of a divalent hcp metal due to spin-orbit coupling. Diagram (a) shows the "without spin" case and (b) the surface in the second band when spin-orbit coupling is taken into account.

Fermi surface corresponding to the holes in the second band in Mg,[3] Zn,[13,14] and Cd,[13] which without spin-orbit coupling may sustain open orbits[15] with general directions only *perpendicular* to the c axis [Fig. 3(a)], with spin-orbit coupling changes its topology [Fig. 3(b)] so as to permit open trajectories *parallel* to the c axis.

However, because of the smallness of some of these gaps, magnetic breakdown effects[16] must be expected to appear at relatively low magnetic fields, in which case the electron trajectory will ignore the gap, restoring the previous "without-spin" topology. This is certainly the case for Mg where relatively small fields of the order of 200 G must be enough to produce breakdown.

To estimate the values of the splittings for the other hcp metals it must be emphasized that the values at H_1 and H_3 come almost exclusively from the "atomic" part of the wave function, while the much smaller H_2 splitting arises from lattice effects. Therefore, the H_1 and H_3 gaps for Be, Zn, Cd, and Tl must be of the order of 0.05, 9.5, 28, and 129 times the corresponding values for Mg. These figures are obtained from the term values of the configurations $2s2p\,^3P_J$, $4s4p\,^3P_J$, $5s5p\,^3P_J$, and $6s^26p\,^2P_J$ of the respective atoms.[12]

No good estimate of the H_2 splittings can be made since these depend critically on the behavior of the wave functions and potential throughout the crystal and not only near the ion sites. Even for magnesium the computed value may be in error by orders of magnitude. The contribution from the plane-wave part of the wave function is very important here, and the assumption of spherical potentials around each nucleus as well as the truncation of the series to include only six OPW's are indeed bad approximations for this level. Nonetheless they must be in general orders of magnitude smaller than H_1 and H_3.

The existence of the spin-splittings near H has been observed experimentally several times in[17] Zn and[17,18] Cd by means of the de Haas–van Alphen effect and ultrasonic attenuation. The first method shows the existence, for magnetic fields parallel to the c axis, of two closed orbits of very similar area arising from the lifting of the spin degeneracy near H. The ultrasonic absorption for magnetic fields perpendicular to the c axis shows the existence of an open orbit parallel to the c axis which can only exist in the presence of spin-orbit effects.

Finally, no splitting close to H has been found in Mg. This is due to the smallness of the gaps, because the relatively low fields necessary to produce magnetic breakdown make unlikely any experimental determination in the nonbreakdown region. However, spin-orbit effects may be of considerable importance in the interior of the zone, where accidental degeneracies of the "without-spin" bands are removed. Theoretical[16] and experimental[19,20] evidence for such an effect has been found.

We would like to acknowledge a very fruitful discussion with W. A. Harrison.

[13] W. A. Harrison, Phys. Rev. **118**, 1190 (1960).
[14] W. A. Harrison, Phys. Rev. **126**, 497 (1962).
[15] L. M. Lifschitz, M. Ya. Azbel, M. I. Kaganov, Zh. Eksperim. i Teor. Fiz. **30**, 220 (1955) [translation: Soviet Phys.—JETP **3**, 143 (1956)]; I. M. Lifschitz and V. G. Peschanskii, Zh. Eksperim. i Teor. Fiz. **35**, 1251 (1958) [translation: Soviet Phys.—JETP **8**, 875 (1959)].
[16] M. H. Cohen and L. M. Falicov, Phys. Rev. Letters **7**, 231 (1961).
[17] A. S. Joseph, W. L. Gordon, J. R. Reitz, and T. G. Eck, Phys. Rev. Letters **7**, 334 (1961).
[18] J. D. Gavenda and B. C. Deaton, Phys. Rev. Letters **8**, 208 (1962).
[19] M. G. Priestley. Thesis submitted to the University of Cambridge, England, 1961 (unpublished).
[20] R. W. Stark, T. G. Eck, W. L. Gordon, and F. Moazed, Phys. Rev. Letters **8**, 360 (1962).

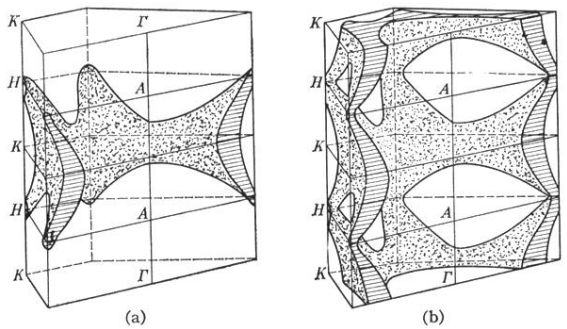

FIG. 3. The change in the connectivity properties of a divalent hcp metal due to spin-orbit coupling. Diagram (a) shows the "without spin" case and (b) the surface in the second band when spin-orbit coupling is taken into account.